but do not prove the validity of, the Renkin equation for correlating the hindrance effect in microporous membranes. On the average, our data are about 4 percent below the values predicted by the Renkin equation. The data seem to be randomly scattered about the line, and there is no trend for the results for individual membranes, an indication that the correlation does not change with larger pores. The dimensionless ratio R_s/R_p seems to be a valid parameter for characterizing the hindrance effect over this range of pore sizes. Within the scatter of the experimental data, other empirical equations such as

$$\frac{\mathcal{D}_m}{\mathcal{D}_0} = \left(1 - \frac{R_s}{R_p}\right)^n$$

where n is about 4, correlate the data equally well.

Although the mechanism for the apparent drag on molecules as they pass through holes of molecular dimensions has not yet been determined, there can be no question that this effect does exist. In the experiments cited here, pore sizes were outside the range postulated for some natural membranes, such as the red blood cell, but within the range of pore sizes indicated for the kidney glomerulus (70 to 100 Å) (*14*). We have shown that the Renkin equation or similar correlations can be used with some confidence to evaluate pores in natural membranes (*15*).

On the basis of the data presented here, one can estimate the reduction in aqueous diffusion rates of solutes in porous materials, where the pores are of molecular dimensions, with a greater degree of confidence than has been possible heretofore. However, some knowledge of the structure of the porous material is required for such calculations, that is, average pore size, void fraction, and tortuousity. On the other hand, if the structure of the porous material is not well characterized, that is, if void fraction, pore size, or tortuousity is not known, then the use of diffusion studies with probe molecules and the correlation as presented in Fig. 3 can lead to information on the unknown parameter.

ROBERT E. BECK
JEROME S. SCHULTZ
Division of Chemical Engineering, University of Michigan, Ann Arbor

References and Notes

1. W. Ruhland and C. Hoffman, *Planta* **1**, 1 (1925); W. Wilbrandt, *Arch. Gesamte Physiol. Menschen Tiere (Pfluegers)* **241**, 302 (1938–39); J. W. Green, *J. Cell Comp. Physiol.* **33**, 247 (1949); J. R. Pappenheimer, E. M. Renkin, L. M. Borrero, *Amer. J. Physiol.* **167**, 13 (1951); J. R. Pappenheimer, *Physiol. Rev.* **33**, 307 (1953); C. V. Paganelli and A. K. Solomon, *J. Gen. Physiol.* **41**, 259 (1957); O. Giebel and H. Passow, *Arch. Gesamte Physiol. Menschen Tiere (Pfluegers)* **271**, 378 (1960).
2. L. C. Craig, *Science* **144**, 1093 (1964).
3. G. K. Akers, *Advan. Protein Chem.* **24**, 343 (1970).
4. E. Manegold, *Kolloid Z.* **49**, 372 (1929); J. D. Ferry, *J. Gen. Physiol.* **20**, 95 (1936); *Chem. Rev.* **18**, 373 (1936); H. Spandau and W. Gross, *Chem. Ber.* **74B**, 362 (1941); G. K. Akers and R. L. Steere, *Biochim. Biophys. Acta* **59**, 137 (1962); B. M. Uzelac and E. L. Cussler, *J. Colloid Interface Sci.* **32**, 487 (1970).
5. E. M. Renkin, *J. Gen. Physiol.* **38**, 225 (1954).
6. R. L. Fleischer, P. B. Price, R. M. Walker, *J. Appl. Phys.* **33**, 3407 (1962); *Rev. Sci. Instrum.* **34**, 510 (1963); R. L. Fleischer, P. B. Price, E. M. Symes, *Science* **143**, 249 (1964).
7. W. J. Petzny and J. A. Quinn, *Science* **166**, 751 (1969).
8. R. E. Beck, thesis, University of Michigan (1969).
9. The tortuousity is calculated from the average angle of incidence of the fission tracks with respect to the surface of the mica membrane. The fission foil was placed about 6 inches (15.2 cm) from the mica surface; the maximum angle of incidence of the fission fragments was about 15° from the normal, and the weighted average was about 8°.
10. Water flow through the membranes was measured under a 2-cm H_2O pressure gradient. Average pore radius was calculated from Poiseuille's law
$$R_p = \left(\frac{8QL\mu}{\pi NA\Delta p}\right)^{1/4}$$
where Q is the total water flow rate (in cubic centimeters per second), L is the membrane thickness, μ is the viscosity, N is the number of pores per unit membrane area, A is the area of the membrane, and Δp is the pressure gradient.
11. V. Levich, *Physicochemical Hydrodynamics* (Prentice-Hall, Englewood Cliffs, N.J., 1962).
12. Millipore (nominal pore diameter, 0.45 μm; membrane thickness, 25 μm; Millipore Co.) and Nucleopore (pore diameter, 0.8 μm; membrane thickness, 8 μm; General Electric Co.) membranes have large pores and therefore no restricted diffusion effects and relatively low diffusion resistance. The permeability (P_m) of these membranes was estimated from their physical properties, and subtracted from the overall diffusion resistance measured with each of the test solutes. The difference was attributed to liquid film resistances, that is,
$$P_l = 2/(P_o^{-1} - P_m^{-1})$$
Values for P_l were obtained for each of the test solutes in the diffusion cell under the same flow conditions as for the mica membranes. Estimates of the liquid film permeability (P_l) from measurements with these large pore membranes and from the electrochemical method agreed to within ± 5 percent.
13. Diffusion coefficients of solutes within the membrane pores were calculated by means of:
$$\mathcal{D}_m = \frac{P_m L}{\pi R_p^2 N}$$
14. D. A. Goldstein and A. K. Solomon, *J. Gen. Physiol.* **44**, 1 (1960); G. Wallenius, *Acta Soc. Med. Upsal. Suppl. 4* (1954); G. Giebisch, H. D. Lausen, R. F. Pitts, *Amer. J. Physiol.* **178**, 168 (1954).
15. A. K. Solomon, *J. Gen. Physiol.* (Suppl.) **51**, 335 (1968).
16. L. G. Longsworth, *J. Amer. Chem. Soc.* **75**, 5705 (1953).
17. F. J. Joubert and T. Haylett, *J. S. Afr. Chem. Inst.* **15**, 48 (1962).
18. Supported in part by PHS grant GM 15152.

12 May 1970; revised 24 July 1970 ■

Coral Skeletons: An Explanation of Their Growth and Structure

Abstract. *Coral skeletons are constructed of aragonitic crystals organized into fan systems. A theoretical model for the growth of such fan systems, which depends upon competition between crystals for space in which to grow, is corroborated by vital staining with sodium alizarinesulfonate. Fan systems of crystals compete with each other to form larger fan systems until large, relatively stable fans are produced. It is these relatively stable fan systems that have been observed in optical thin sections of coral skeletons.*

The microscopic appearance of coral skeletons is well known since it forms the basis of coral systematics (*1*). The basic unit of the skeleton is considered to be the sclerodermite, a group of fibers which fan out from a point called the center of calcification. Sclerodermites often grow vertically to produce a trabecula in which the fibers radiate outward and upward from a central axis which is supposed to be an elongated center of calcification. In most corals only the sclerosepta are trabecular. The sclerosepta comprise a palisade of trabeculae, each of which terminates in a dentation or tooth on the upper surface of the scleroseptum. Sorauf (*2*) and Wise (*3*) have shown that the fibers seen in optical section are acicular crystals, and both have confirmed that the crystals are normally organized into sclerodermites. They have shown that sclerodermites are fundamental to the structure of the dissepiments. I have found similar, though less organized, sclerodermites in the epitheca of three West Indian corals, and Wainwright (*4*) has described the development of sclerodermites on the basal plate of *Pocillopora damicornis*. Thus, all the parts of coral skeletons, so far examined, are built of crystals arranged in three-dimensional fans, and it seems appropriate to attempt to explain the development of these fans in terms of the physics of crystal growth.

I have followed the growth of sclerodermites and trabeculae by staining growing crystals red with sodium alizarinesulfonate, a dye used for vitally staining bone (*5*). When living corals and washed coral skeletons were placed in seawater containing about 20 mg of alizarine per liter, the washed skeletons were only stained on freshly damaged surfaces, whereas the skeletons of liv-

ing corals were stained generally. Living corals were lightly stained after 1 hour in the solution; longer exposures caused more intense staining. If living corals were subsequently returned to running seawater, unstained deposits were laid over stained areas. Repeating this procedure caused multiple staining. Microscopic examination of ground thin sections of multiply stained skeletons showed bands of stain in concentric layers around each center of calcification. Duration of staining was varied from 3 to 24 hours, and the periods between staining varied from 6 hours to 3 days. The relative widths of stained bands, and the distances between them, indicated the order of staining and hence the direction of growth of the crystals. Crystals were found to grow out from each center of calcification until they met crystals that were growing out from adjacent centers, at which point mutual interference prevented further growth.

Bryan and Hill attempted to explain the trabecular structure of the sclerosepta in terms of the vertical growth of a line of such mutually interfering centers (*6*). They noted that the crystals in dentations are oriented perpendicularly to the surface and suggested that new crystals are initiated at the tip of the dentation and begin to grow outwards and upwards. Crystals would continue to grow out until at the base of the dentation they met crystals from adjacent trabeculae. However, the tip of each dentation is not a single, inverted cone-shaped point but is made up of several spikes (Fig. 1A), and their explanation does not account for the divergence of linear groups of sclerodermites from the axis of the trabeculae to emerge on the sides of sclerosepta as small granulations.

When the several points at the tips of dentations in *Isophylia sinuosa* were examined in thin section, it was found that each is a three-dimensional fan of crystals. Thus the trabeculae in *I. sinuosa* are not an extension of a single sclerodermite in the vertical plane; instead the axis of each trabecula is composed of a number of sclerodermites growing upwards together. Using the techniques developed for electron microscopy, I embedded a number of specimens of *I. sinuosa* and *Mycetophyllia lamarkiana* in araldite, and was able to grind thin sections of the skeleton with the tissue in place. I found that at the tip of each dentation the tissue was lifted away from the skeleton to create a cavity into which the sclerodermites projected. This suggests that the animal was creating an environment in which crystal growth would occur. Wells has pointed to other evidence which suggests that calcification takes place most rapidly where the calicoblastic, or calcium-secreting, layer is lifted away from the skeleton (*7*). Thus it is possible that the animal brings about skeletal growth by generating a supersaturated solution of calcium carbonate above the skeleton.

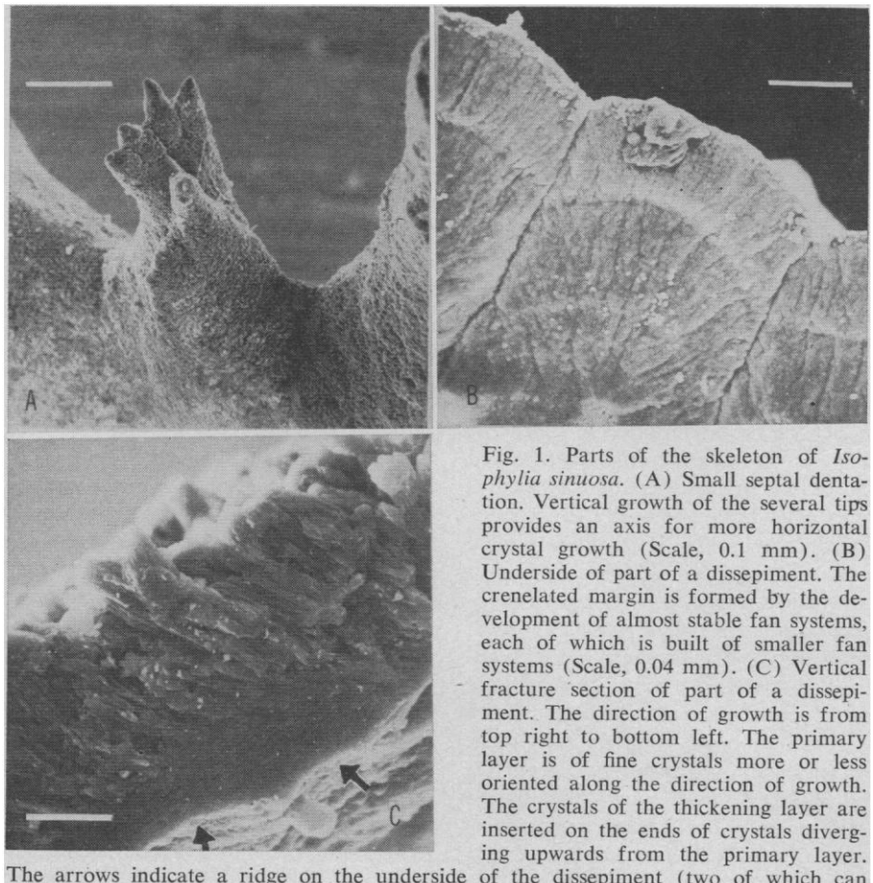

Fig. 1. Parts of the skeleton of *Isophylia sinuosa*. (A) Small septal dentation. Vertical growth of the several tips provides an axis for more horizontal crystal growth (Scale, 0.1 mm). (B) Underside of part of a dissepiment. The crenelated margin is formed by the development of almost stable fan systems, each of which is built of smaller fan systems (Scale, 0.04 mm). (C) Vertical fracture section of part of a dissepiment. The direction of growth is from top right to bottom left. The primary layer is of fine crystals more or less oriented along the direction of growth. The crystals of the thickening layer are inserted on the ends of crystals diverging upwards from the primary layer. The arrows indicate a ridge on the underside of the dissepiment (two of which can be seen in Fig. 1B) that results from increased crystal growth in the primary layer during daylight (Scale, 0.01 mm).

In a supersaturated solution, in which crystals of the dissolved solid are already present, crystal growth may proceed in two ways. The solution will tend towards saturation by losing molecules to the lattices of the crystals present. These crystals will then grow while maintaining their original orientations. This is called syntaxial growth (or epitaxial growth). However, if the solution is sufficiently supersaturated, new crystals may be nucleated on the surfaces of the original crystals. Once nucleated, these crystals will grow syntaxially but their orientation will not depend upon the orientation of the original crystals. This type of growth, which usually produces a mass of randomly oriented crystals, is termed nonsyntaxial. The relationship between the two types of growth depends on the degree of supersaturation of the solution in which they are growing. The more the solution is supersaturated, above the level at which nucleation takes place, the greater the amount of nucleation. Examination of fan systems with the scanning electron microscope reveals that new crystals grow between the original crystals as the fan develops and that in all cases the crystals are straight though very slightly wedge-shaped. Thus the question arises of the way in which nonsyntaxial growth is constrained to produce a fan of crystals rather than a random mass.

It is possible to explain the production of fan systems of crystals as a physical rather than an organic phenomenon. The first sclerodermites that the animal produces are formed as part of the basal plate laid down by the newly settled larva. The initial deposit is probably a layer of calcite 1 to 2 μm thick (*4*). If a supersaturated solution of calcium carbonate suitably buffered with organic molecules and inorganic ions to favor the precipitation

of aragonite (*8*) is formed between the calicoblast and the calcitic primary plate, then nucleation will take place on the primary plate. At first the crystals will be randomly oriented. However, aragonitic crystals grow fastest along their *c*-axis, producing the typical acicular form. Crystals with their *c*-axis oriented perpendicular to the primary plate will be able to grow indefinitely, whereas crystals with their *c*-axes more horizontally oriented will eventually be prevented from extending by interference with other crystals. Because the growth of one crystal may prevent the further growth of another crystal, it may be said that the crystals compete for space in which to grow. The space for which they compete is the cavity beneath the calicoblast which contains the supersaturated solution. New crystals may be nucleated on any surface within this cavity but will only be able to extend along their *c*-axes as long as they continue to extend into the cavity and provided that other crystals do not grow across their path.

Thus the crystals formed on the primary layer of the basal plate will quickly become oriented more or less perpendicularly, but not exactly perpendicularly, to the primary plate. Because the crystals will not all terminate in the same plane, a crystal nucleated near the end of a projecting crystal, and growing nearly perpendicularly, could cut off the syntaxial growth of other, less projecting crystals that are growing perpendicularly. As Fig. 2 shows, this will only happen where the new crystal has nearly the same orientation as the previously formed crystals. The tendency of crystals to diverge from the optimum axis of growth gives rise to three-dimensional fans. These fans will develop all over the primary plate, and adjacent fans will compete for space in which to develop. If one fan grows faster than another, the smaller fan will be forced to grow more and more away from the optimum axis. In a horizontal layer of fans, the smaller fans will quickly be overgrown by fans around them. The successful fans will then meet and further competition will take place. Because the fans become larger at each stage, it will become increasingly more difficult for some fans to overgrow others. Eventually almost stable fan systems will develop—these are the sclerodermites of the basal plate. They grow upwards side by side with interference occurring at their

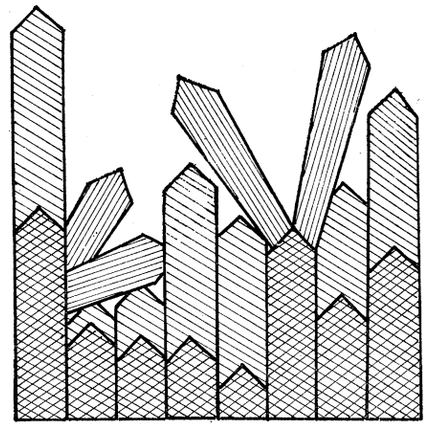

Fig. 2. Diagrammatic representation of syntaxial growth (diagonal shading) and nonsyntaxial growth (linear shading) on crystals present (cross-hatched shading) in a supersaturated solution.

margins. Figure 1B shows the development of a sheet of fan systems on the underside of a dissepiment. The figure may be considered as a two-dimensional representation of the development of sclerodermites in the basal plate.

The sclerosepta grow from the basal plate. By limiting the extent of the cavity beneath itself, the animal may accentuate the upward growth of groups of sclerodermites so that they form projections. If such projections were arranged in a line, syntaxial growth behind each tip would result in a laminar septum, in the manner described by Bryan and Hill (*6*). Those axial sclerodermites which lost the competition would be forced to grow more and more laterally. Subsequent growth would cause some of these to emerge on the side of the septum as granulations. The final form of a septum would depend upon the initial spacing of the cavities above the basal plate and the amount of syntaxial growth that occurred behind the tip of each dentation. In all cases the final unit of fanning is stable because it is separated from its neighbors by tissue. In most corals, this final unit is the trabecula, but in mussid corals it is a fan of trabeculae (*9*).

Coral skeletons are built of four elements, the basal plate, the septa, the epitheca, and the dissepiments. The epitheca is an upward growth of the basal plate to form a wall that invests the whole skeleton. The scanning electron microscope shows that it has a structure similar to that of the basal plate. It is composed of somewhat disorganized sclerodermites inserted on a primary layer of a different crystal structure. The dissepiments are horizontal bulkheads placed between the septa to form a false floor to the skeleton. They are formed periodically and serve to strengthen the skeleton and to isolate regions of it that are no longer occupied. Dissepiments form by the growth of plates, from the sides of adjacent septa, to fuse centrally.

The formation of dissepiments in hermatypic corals provides a test of competitive crystal growth. Alizarin staining of specimens of *Isophylia* at different times of the day shows that the dissepiments grow as thin plates which are thickened on their upper surface, mainly during the day. Daytime additions to the edges of the plates form the growth lines noted by Wells (*7*). The electron stereoscan shows the dissepiment to be two-layered. In Fig. 1C, the lower, or primary, layer is a single fan of crystals which grows outwards from the septum. The upper, or thickening layer, arises by continued growth of crystals diverging upwards from the primary layer. At regular intervals along its length, the primary layer increases and decreases in thickness. Comparison of photomicrographs of stained dissepiments with electron stereographs of the same dissepiments, shows that the bulges in the primary layer correspond to daytime additions to the edge of the dissepiment.

Goreau has shown that light increases the rate of calcification of hermatypic corals by its action on the symbiotic algae present in their tissues (*10*). The algae aid calcification by the removal of carbon dioxide from the reaction:

$$Ca^{2+} + 2HCO_3^- \rightleftharpoons CaCO_3 + H_2O + CO_2$$

Thus light will increase the supersaturation of the solutions beneath the coral. This will affect the growth of crystals. Increased nucleation of new crystals will cause the fans to spread more rapidly, and all crystals will grow faster. In most fan systems this effect will be masked by subsequent growth. In the primary layer of the dissepiment it is only partially masked by the thickening layer. The regular bulges in the primary layer are caused by a more divergent growth of crystals to a greater length, indicating that, during the day, the fan has spread more rapidly and the crystals have grown faster than at night.

Ridges on the underside of the dissepiment, caused by bulges on the primary layer, have been noted in *Favia favus* and *I. sinuosa*. The growth lines

that correspond to these ridges probably result from increased disorganization of the structure of daytime additions which increases the intercrystal spaces and causes the deposit to be more opaque. Opaque growth lines are only found in hermatypic corals. They are not formed when specimens are grown in the dark for several days. It follows from the above explanation of growth and structure of the skeleton that growth lines, of the nature and form of those described, would be present in the primary layer of the dissepiment.

The formation of fan systems is not limited to scleractinian corals. Most fossil corals show remnants of fan systems. The sclerosponges, which are apparently modern representatives of the stromatoporoids, have a skeletal structure very similar to that of corals (*11*). Calciferous spicules in many sponges and octocorals have a similar organization. Some recent stereoscan photographs of mollusk shells (*12*) show distinct fan systems. It is probable that the principle of competitive crystal growth may be used to explain the form and microstructure of many types of skeleton which include acicular crystals in their structure.

DAVID J. BARNES

Discovery Bay Marine Laboratory, Jamaica, West Indies, and School of Physics, University of Newcastle upon Tyne, Newcastle upon Tyne, England

References and Notes

1. J. W. Wells, in *Treatise on Invertebrate Paleontology*, R. C. Moore, Ed. (Univ. of Kansas Press, Lawrence, 1956), part F, p. 328.
2. J. E. Sorauf, Abstr. *Proc. Geol. Soc. Amer.* **7**, 210 (1969).
3. S. W. Wise, Jr., *ibid.*, p. 241.
4. S. A. Wainwright, *Quart. J. Microscop. Sci.* **104**, 169 (1963).
5. D. A. N. Hoyte, *J. Anat.* **94**, 432 (1960).
6. W. H. Bryan and D. Hill, *Proc. Roy. Soc. Queensland* **52**, 78 (1941).
7. J. W. Wells, in *Stratigraphy and Paleontology*, K. S. W. Campbell, Ed. (Australian National Univ. Press, Canberra, 1969), p. 17.
8. J. L. Wray and F. Daniels, *J. Amer. Chem. Soc.* **79**, 2031 (1957); Y. Kitano and D. W. Hood, *Geochim. Cosmochim. Acta.* **29**, 29 (1965).
9. A detailed analysis of the structure and growth of coral skeletons is in preparation.
10. T. F. Goreau, *Biol. Bull.* **117**, 239 (1959b).
11. W. D. Hartman and T. F. Goreau, *Symp. Zool. Soc. London* **25**, 205 (1970).
12. S. W. Wise, *Trans. Amer. Microscop. Soc.* **87**, 411 (1968), figures 5, 7, and 8; *ibid.*, p. 419, figure 9. These photographs show that in some mollusk shells, the prismatic layer is a layer of crystal fans, probably initiated on the periostracum, which becomes overlain by the nacreous layer.
13. I thank Dr. L. S. Land for his help in developing the above principle, and Sir Maurice Yonge and Dr. J. W. Wells for their comments on the manuscript. Supported by the Natural Environment Research Council of the United Kingdom as a research studentship and by an NSF grant to Prof. S. K. Runcorn.

17 September 1970

Mars: Detection of Atmospheric Water Vapor during the Southern Hemisphere Spring and Summer Season

Abstract. *Water vapor was found to reappear in the atmosphere of Mars during its southern hemisphere spring and summer season, with a maximum vertical column abundance of 45 to 50 microns of precipitable water averaged over the entire planet. Although the spring-summer seasons for each hemisphere are generally symmetrical with respect to the appearance of water vapor, the data suggest that water vapor may appear later in the season and in slightly larger amounts during the southern hemisphere spring-summer.*

Small amounts of water vapor (up to a few tens of microns of precipitable H_2O in a vertical column) have been reported in the atmosphere of Mars during three of the past four oppositions; in the most recent of these oppositions (1969), the amount and quality of the spectroscopic data were sufficient to establish its presence conclusively. However, all of these previous successful determinations of Martian water vapor have been made when Mars had an orbital longitude L_s of about 60° to 140° (*1*)—that is, during the same spring-summer "wet season" of the Martian northern hemisphere when the north polar cap was receding. Although it is plausible to assume that the situation would be symmetrical with respect to recession of the south polar cap, various factors including the substantial eccentricity of the Martian orbit might produce appreciably different behavior. It is thus of interest that we have recently been able to obtain a number of spectra of the 8200-Å band of H_2O taken at times when Mars had orbital longitudes (L_s) in the range of 250° to 350°, which corresponds to spring-summer in its southern hemisphere.

To set these observations in context, the first true spectroscopic detection of water vapor on Mars was made in 1963 from a single Mount Wilson plate taken at $L_s = 76°$ (*2*, *3*). Measurements of spectra obtained at McDonald Observatory and Lick Observatory during the 1964–65 apparition of Mars, which covered $5° < L_s < 122°$, indicated a definite variation in the water vapor abundance with Martian season, and also with areographic position on the disk of Mars (*4*). The search for water vapor was fruitless during the 1966–67 apparition because of limited observing programs and poor terrestrial observing conditions when the Doppler shift was favorable. In several studies (*5*) made at the McDonald Observatory during the first half of the 1969 apparition ($L_s = 80°$ to 150°, spring-summer in the Martian northern hemisphere) with the improved coudé spectrograph of the 82-inch (207-cm) Struve reflector and the newly installed 107-inch (268-cm) reflector with its coudé spectrograph, the date of reappearance of H_2O in the late spring for the northern hemisphere was established and an average abundance for the whole planet of 20 to 35 μ of precipitable water was obtained. Several of the 82- and 107-inch spectra have good enough areographic resolution to show (*5*, *6*) that the water vapor varied across the disk of the planet from a maximum in the northern hemisphere, where the polar cap was receding, to a minimum in the southern hemisphere.

The first report on attempts to detect water vapor subsequent to the blind opposition period (zero Doppler shift) centered on June 1969 was presented in a detailed review of the history of Martian water vapor studies (*7*). Since the 1969 opposition occurred near the start of Martian southern hemisphere spring when the sub-Earth point was going south, the spectra taken after opposition ($L_s = 190°$ to 340°) refer mainly to the spring and summer season in the southern hemisphere. The prediction was made (*4*, *7*) that water vapor should reappear when the south polar cap had receded to about the

Table 1. Measured water vapor lines on plates C6670, C6676, and C6743 and the average abundance of water vapor determined for each plate.

Wavelength (Å)	Equivalent width (mÅ)		
	Plate C6670	Plate C6676	Plate C6743
8164.54	7.5	8.5	
8169.995	7.5	6.0	5.5
8189.272	7.5	8.0	8.0
8193.113	7.5	10.0	
8197.704	5.5	6.0	
8226.962	7.0	4.5	
8256.515	13.0	12.5	12.5
8282.024		4.5	6.0
Average	7.9	7.5	8.0
Abundance (μ)	45 ± 11	44 ± 9	50 ± 15